Continuous Electroreduction of CO_2 to Formate Using Sn Gas Diffusion Electrodes

Andrés Del Castillo, Manuel Alvarez-Guerra, and Angel Irabien
Dept. de Ingenierías Química y Biomolecular, ETSIIT, Universidad de Cantabria, Avda. Los Castros s/n. 39005, Santander, Spain

DOI 10.1002/aic.14544
Published online July 5, 2014 in Wiley Online Library (wileyonlinelibrary.com)

Electrochemical valorization may be a strategy for mitigating climate change, as the process allows for CO_2 to be converted into industrially useful chemicals. The aim of this work is to study the influence of key variables on the performance of an experimental system for continuous electroreduction of CO_2 to formate with a gas diffusion electrode (GDE) loaded with Sn. A 2^3 factorial design of experiments at different levels of current density (j), electrolyte flow rate/electrode area ratio (Q/A ratio) and GDE Sn load was followed. Higher rates and concentrations (i.e., $1.4{\cdot}10^{-3}$ mol m^{-2} s^{-1} and 1348 mg L^{-1} with efficiencies of approximately 70%) were obtained with GDEs than with plate electrodes. The statistical design of experiments demonstrated that the Sn load had the most significant effect on rate and efficiency. However, despite these promising results, further research is required to optimize the process. © 2014 American Institute of Chemical Engineers *AIChE J*, 60: 3557–3564, 2014

Keywords: carbon dioxide, valorization, electrochemical reduction, formate, Sn gas diffusion electrode

Introduction

In the 20th century, population growth and industrialization have resulted in a significant increase in CO_2 emissions into the atmosphere, increasing the greenhouse effect and producing climate change. The majority of this increase in atmospheric CO_2 can be attributed to fossil fuel combustion.[1]

Several strategies are being considered to reduce CO_2 emissions and mitigate climate change, including increasing the efficiency of industrial processes to reduce their energy consumption, using renewable energy or encouraging the manufacture of environmentally friendly products. Aside from long term strategies that involve a drastic change to the current technologies, alternatives based on the capture, storage, and valorization of carbon dioxide have received increased attention.[1,2]

Carbon capture and storage can prevent the emission of CO_2 into the atmosphere, but storage requires energy to capture and transport CO_2 to carbon sinks. Negative public opinion regarding some projects for CO_2 storage may impede the implementation of this technology,[3–5] and sequestration in geological structures such as depleted gas and oil wells runs the risk of a sudden release.[2]

CO_2 valorization appears to be a more interesting strategy[6,7] because this process allows CO_2 to be converted into value-added products. The valorization of CO_2 to carbon neutral renewable fuels and materials is considered a feasible and powerful new approach to mitigate climate change and to reduce CO_2 emissions.[8] As detailed in reviews on CO_2 valorization, CO_2 transformations can be classified into several categories, including chemical, photochemical, electrochemical, biological, or inorganic transformations.[9,10]

Among these transformations, electrochemical reduction is a particularly interesting method as it could allow for intermittent and unpredictable renewable energy (i.e., solar or wind) to be stored in the form of liquid fuels or chemical products.[11] The storage of electricity to balance fluctuations in demand and production cycles is considered to be essential for renewable energies to be used on a large scale, and the electrochemical reduction of CO_2 has been suggested as an excellent future method of storing this intermittent renewable energy as chemical energy.[8,12]

Several papers have studied the reactions and pathways for the electrochemical reduction of CO_2 into products.[13–15] Accounting for problems that still need to be solved, currently the most promising reaction for industrial scales seems to be the electroreduction of CO_2 into formate.[16,17] Formic acid is used in several industries, including the textile finishing, pharmaceutical synthesis, and paper and pulp production industries.[18] Furthermore, formic acid has been reported to be a suitable fuel for fuel cells.[19,20]

The electroreduction of CO_2 to formate has received increased attention over the past few years. Many references in the literature have focused on studies with parallel-plate or filter press flow-by type cells with different electrode configurations (i.e., plate, mesh or particles) based mainly on Pb[21–23] or Sn.[17,24–26] Several recent studies on electrochemical reduction have paid particular attention to new gas diffusion electrodes (GDEs) and the advantages that these electrodes could offer. A GDE is formed by depositing a catalyst over a gas diffusion layer. The main advantages of

Correspondence concerning this article should be addressed to A. Del Castillo at castilloa@unican.es.

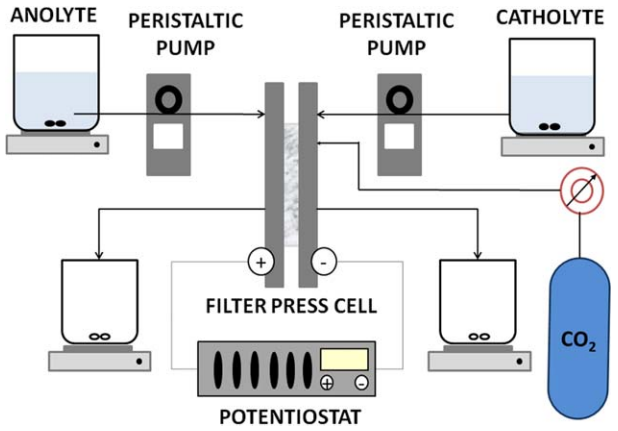

Figure 1. Experimental plant scheme.

[Color figure can be viewed in the online issue, which is available at wileyonlinelibrary.com.]

these electrodes include increased active surface availability and reduced metal use compared to plate electrodes.[27–31] The GDE configuration allows for operation at higher current densities[28,29] and also permits a direct feed of gaseous CO_2 to the cell. Due to these advantages, many works have studied the electroreduction of CO_2 to formate/formic acid with a GDE loaded with different metals, including Pb[27,30,32] and Sn.[16,28,29,33–35] Novel copper rubeanate metal organic frameworks, structured, and porous materials with nanoscale pores, have been used in the electrochemical reduction of CO_2 to formic acid.[36] GDEs have been tested in various electrochemical cell configurations; most notable are recent studies on the electroreduction of CO_2 to formate using filter-press type cells.[16,28,33,35] Moreover, recent studies using Sn particles in GDEs[33,35,37] highlight the growing interest in this type of Sn-based GDEs, which are deserving of further research.

In our research group, previous studies[21,26] determined the influence of key variables on the performance of an experimental system for continuous electroreduction of CO_2 to formate in aqueous solutions under ambient conditions in a filter-press electrochemical reactor with Pb and Sn plate electrodes. The fact that better results were obtained with a Sn plate rather than a Pb plate[26] renewed our interest in Sn as a catalytic material for the electroreduction of CO_2 to formate. Additionally, according to the promising results reported in recent references regarding GDEs, there is interest in studying new cathodes based on a Sn-GDE configuration to improve the performance of continuous electrochemical process to convert CO_2 into formate. Consequently, the aim of this work is to study the influence of key variables on the performance of a process using a GDE prepared with Sn metal catalyst particles in a filter-press electrochemical reactor. A 2^3 factorial design of experiments was carried out to determine the influence of the following variables: current density (j), electrolyte flow rate/electrode area ratio (Q/A ratio), and Sn load on the GDE. Based on results from the factorial experiments, the study was subsequently broadened with additional experiments in an attempt to improve process performance.

Methods

The main elements of the experimental setup and operating conditions were the same as in our previous studies,[21,26] with differences resulting from the use of a GDE cathode instead of a plate. The experimental laboratory system included two tanks, two pumps, a potentiostat/galvanostat, and an electrochemical cell as shown in Figure 1. An aqueous solution of 0.45 mol/L $KHCO_3$ + 0.5 mol/L KCl was used as the catholyte, and a 1 mol/L KOH solution was used as the anolyte. The electrolytes were pumped to the cell by two peristaltic pumps (Watson Marlow 320, Waton Marlow Pumps Group). In the electrochemical cell (Micro Flow Cell, ElectroCell A/S), electroreduction of CO_2 takes place due to the current supplied by the potentiostat/galvanostat (AutoLab PGSTAT 302N, Metrohm).

The cell was a filter-press or parallel-plate type cell and was divided into two compartments by a Nafion 117 membrane as shown in Figure 2. The cell had three inputs (catholyte, anolyte, and CO_2) and two outputs (anolyte and catholyte + CO_2). A Dimensionally Stable Anode [DSA/O_2(Ir-MMO (Mixed Metal Oxide) on Platinum, Electrocell A/S)] plate was used as the counter-electrode. The working electrode was a GDE loaded with Sn. The GDE was manufactured by spreading a catalytic ink over carbon paper (Toray carbon paper, TGP-H-60); this process was adapted from previous procedures described in the literature.[37] The catalytic ink was prepared by dispersing Sn powder (−100 mesh, 99.5%, Alfa Aesar) in a Nafion solution (copolymer PTFE 5% w/w, Alfa Aesar) and deionized water at a Nafion/water ratio of 1:1. Ultrasonic agitation was used to homogenize the mixture for 30 min. The electrodes were dried at ambient conditions for 1 day. Each of the electrodes had a surface area of 10 cm^2. A leak-free Ag/AgCl 3.4 mol/L KCl reference electrode was assembled close to the surface of the working electrode.

Experiments were carried out at ambient temperature and pressure, and the cell was operated in continuous mode. All experiments were performed at galvanostatic conditions (i.e., at a constant current density), meaning that the total amount

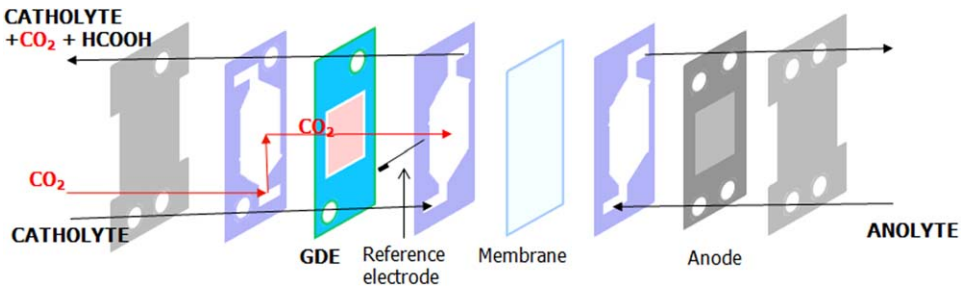

Figure 2. Cell scheme.

[Color figure can be viewed in the online issue, which is available at wileyonlinelibrary.com.]

Table 1. Results of the Factorial Design of Experiments Using Sn-GDE Cathode

Point	Measured Formate Concentration (mg L^{-1})	Sn load[a]	Flow/Area Ratio, Q/A[b]	Current Density, j[c]	Rate·10^4 (mol m^{-2} s^{-1})	Faradaic Efficiency (%)	Normalized Rate [−1, +1]	Normalized Faradaic Efficiency [−1, +1]	Cathode Potential vs. Ag/AgCl (V)	Cell Potential (Absolute Value) (V)
					r	η	$\bar{r}$	$\bar{\eta}$	V_{cat}	V_{cell}
1	55.1	−	−	−	1.17	18.7	−0.99	−0.82	−1.75	2.80
	52.6	−	−	−	1.11	17.9	−1.00	−0.85	−1.70	2.74
	53.9	−	−	−	1.14	18.3	−0.99	−0.83	−1.72	2.76
2	140.6	+	−	−	2.97	47.7	−0.57	0.37	−1.75	2.90
	120.6	+	−	−	2.55	40.9	−0.67	0.09	−1.73	2.87
	160.5	+	−	−	3.39	54.5	−0.48	0.65	−1.73	2.85
3	28.0	−	+	−	2.38	38.3	−0.71	−0.01	−1.72	2.51
	28.6	−	+	−	2.43	39.1	−0.70	0.02	−1.73	2.78
	27.3	−	+	−	2.33	37.5	−0.72	−0.05	−1.74	2.53
4	46.1	+	+	−	3.92	63.1	−0.36	1.00	−1.70	2.77
	41.6	+	+	−	3.54	57.0	−0.44	0.75	−1.68	2.69
	34.6	+	+	−	2.95	47.4	−0.58	0.36	−1.56	2.43
5	120.0	0	0	0	6.40	56.1	0.21	0.72	−1.50	3.15
	105.0	0	0	0	5.60	49.1	0.03	0.43	−1.48	3.15
	114.0	0	0	0	6.08	53.3	0.14	0.60	−1.50	3.16
6	111.9	−	−	+	2.36	14.2	−0.71	−1.00	−1.95	3.60
	131.6	−	−	+	2.78	16.8	−0.62	−0.90	−1.90	3.56
	119.7	−	−	+	2.53	15.2	−0.68	−0.96	−1.96	3.58
7	363.8	+	−	+	7.68	46.3	0.50	0.31	−1.96	2.78
	405.7	+	−	+	8.56	51.6	0.71	0.53	−1.96	2.77
	443.6	+	−	+	9.36	56.5	0.89	0.73	−1.73	2.90
8	37.5	−	+	+	3.19	19.2	−0.52	−0.80	−1.98	3.30
	36.1	−	+	+	3.08	18.6	−0.55	−0.82	−2.05	3.50
	43.4	−	+	+	3.70	22.3	−0.41	−0.67	−2.00	3.70
9	97.7	+	+	+	8.33	50.2	0.65	0.47	−1.89	3.24
	115.6	+	+	+	9.85	59.4	1.00	0.85	−2.00	3.60
	88.9	+	+	+	7.57	45.7	0.48	0.29	−1.98	3.70

[a]Levels for Sn load (mg Sn cm^{-2}): 1.5(+), 0.7(−), 1.1(0)
[b]Levels for flow/area ratio (mL min^{-1} cm^{-2}): 2.3(+), 0.57(−), 1.44(0)
[c]Levels for current density (mA cm^{-2}): 32(+), 12(−), 22(0)

of charge passed at the end of each test was simply the product of the current density (j), the electrode area (10 cm^2), and the time of operation (90 min). Samples were taken at different times of operation (15, 30, 60, and 90 min). Each sample was analyzed in duplicate by ion chromatography (Dionex ICS 1100 equipped with an AS9-HC column, using a solution of Na_2CO_3 (4.5 mmol/L) as the eluent at a flow rate of 1 mL min^{-1} and a pressure of approximately 13.79 MPa) to quantify the concentration of formate produced. An average concentration was obtained for each experiment. Due to the variability of the process, three experiments were performed for each point in the factorial design. The standard deviations of all the experiments were below 15%.

The performance of the process was assessed using the rate of formate production and the Faradaic efficiency. The rate of formate production was defined as the quantity of formate obtained per unit of cathode area and unit of time. The Faradaic efficiency is the percentage of the total charge supplied that is used to produce formate,[38] which is widely used as a measure of the selectivity of the process for a given product.[6]

Results and Discussion

Factorial design of experiments

To analyze the effects of current density (j), electrolyte flow per electrode area (Q/A ratio) and Sn load on the formate rate and efficiency, a 2^3 factorial design of experiments was used following the same approach described in previous studies.[21,26] The two levels for each variable were 12 and 32 mA cm^{-2} for j; 0.57 and 2.3 mL min^{-1} cm^{-2} for the Q/A ratio; and 0.7 and 1.5 mg Sn cm^{-2} for the Sn load. In addition, a center point involving medium values within the ranges of the 3 factors (22 mA cm^{-2}, 1.44 mL min^{-1} cm^{-2}, and 1.1 mg Sn cm^{-2}) was added to evaluate the curvature.

The results of the experiments using the GDE are summarized in Table 1. Minitab 15.6 was used to analyze the results of the factorial experiments. First, the 2^3 factorial design without the center point was analyzed; the center point was then added in a second analysis. To remove the influence of the variables' absolute values in these analyses, the factors (j, Q/A, and Sn load) and the responses (rate of formate production and Faradaic efficiency) were normalized in the range [−1, 1].

Table 2 shows the statistical analyses of the 2^3 experiments with the center point excluded. The Sn load in the GDE has the greatest main effect on both rate and efficiency. These effects are positive and significant for both responses, which means that the effect of increasing the Sn load per cm^2 resulted in increases of 0.81 and 1.17 (on the normalized scale) in the rate and efficiency, respectively.

Both Sn load and j have significant high and positive main effects of similar magnitude on the rate. The effect of Q/A ratio on rate and efficiency is also positive, but this effect is smaller and insignificant.

It is notable that j has a negative effect on the Faradaic efficiency, a behavior also observed in previous studies with Pb and Sn plates.[21,26] However, this main effect is smaller

Table 2. Statistical Analysis of the 2^3 Factorial Experiments with Sn-GDE Cathode, $\bar{r}(-)$ is the Normalized Rate of Formate Production and $\bar{\eta}(-)$ is the Normalized Faradaic Efficiency

	Sn Load, X_1			Current Density, j, X_2			Flow/Area Ratio, Q/A, X_3			Regression Model: Response $= \beta_0 + \beta_1 X_1 + \beta_2 X_2 + \beta_3 X_3$				
										Coefficients (95% Confidence Bounds)				
	Main Effect	Error	P^a	Main Effect	Error	P^a	Main Effect	Error	P^a	β_0	β_1	β_2	β_3	R^2
$\bar{r}(-)$	0.810	0.02678	0	0.746	0.02678	0.015	0.146	0.02678	0.015	-0.311 ± 0.125	0.405 ± 0.125	0.373 ± 0.125	0	0.800
$\bar{\eta}(-)$	1.174	0.04069	0	-0.219	0.04069	0.016	0.337	0.04069	0	0	$0.587 \pm 3.6 \cdot 10^{-5}$	$-0.109 \pm 3.6 \cdot 10^{-5}$	$0.168 \pm 3.6 \cdot 10^{-5}$	0.857

[a]Significant ($\alpha = 0.05$) if $P < 0.05$.

for GDEs than for Pb and Sn plates (-0.219 on GDE vs. -1.295 on Pb plates and -1.379 on Sn plates).

As shown in Table 2, linear regression models can also be used to express the results of a factorial design. The highest values of β corresponded to the parameter that multiplies the Sn load, demonstrating the variable's significant influence, as has been shown previously. The negative coefficient for current density in the efficiency expression indicates that current density has a negative influence on efficiency. Low values of β parameters that multiply Q/A indicate the limited influence of this variable, especially on rate. Finally, the R^2 values for the rate and efficiency regression models were low (0.814 and 0.864, respectively), suggesting that a more complex mathematical model is necessary to fit these results.

Adding the center point allows for the testing of curvature (Table 3), a measurement of the difference between the average of the center-point response and the average of the factorial points.[39] A curvature of 0.6351 for efficiency suggests a nonlinear performance relationship. The curvature for rate is also significant but lower than the curvature for efficiency.

To allow for a clearer visualization of the influences detected by the statistical analysis, the average absolute values of the rate of formate production and the Faradaic efficiency at each of the 2^3 experimental points investigated are represented in Figure 3.

In Figures 3a, b, it can be seen that a slight increase in rate occurs when j is increased in the GDE with 0.7 mg Sn cm^{-2} at the two levels of Q/A (Figure 3a). However, this increase in rate comes at the expense of a decreased Faradaic efficiency. Especially at a Q/A ratio of 2.3 mL min^{-1} cm^{-2}, the efficiency decreased from 40 to 20% (Figure 3b) when j was increased from the low to the high level in the GDE with a low Sn load.

An interesting result was obtained for a high Sn load, where the current density has much more influence. The rate of product formation almost doubled for both of the Q/A ratios studied when j was increased from 12 to 32 mA cm^{-2} (i.e., the rate increased from approximately $3 \cdot 10^{-4}$ to $8.5 \cdot 10^{-4}$ mol m^{-2} s^{-1}; Figure 3a). It should be noted that this significant increase in the rate of formate production was obtained without a significant decrease in efficiency: as shown in Figure 3b, the efficiency remained approximately 50%.

Figures 3c, d allow the influence of Q/A on rate and efficiency to be visualized more clearly. Contrary to expectations based on previous work with Sn electrodes,[26] the Q/A ratio used in the experiments with Sn-GDEs hardly affected process performance. For a Sn load of 0.7 mg Sn cm^{-2}, only a slight increase in rate and efficiency was obtained when Q/A was increased, while increasing Q/A had no effect on rate or efficiency for a high Sn load (Figures 3c, d). These results are in good agreement with the statistical analysis of the factorial design, where the influence of Q/A ratio was determined to be much more limited than the other two variables studied (j and Sn load).

As indicated by the statistical analysis, the Sn load had the most significant effect on rate and efficiency. Using the GDE with 1.5 mg Sn cm^{-2} allowed an efficiency 30 points in percentage higher than the GDE with 0.7 mg Sn cm^{-2} to be achieved. In addition, using the higher Sn loading had a positive effect on rate, particularly for a current density of 32 mA cm^{-2}. With this configuration and current density, a rate of $8.5 \cdot 10^{-4}$ mol m^{-2} s^{-1} with an efficiency of 50% was obtained.

Table 3. Statistical Analysis of the 2^3 + Center Point (0,0) Factorial Experiments with Sn-GDE Cathode, $\bar{r}(-)$ is the Normalized Rate of Formate Production and $\bar{\eta}(-)$ is the Normalized Faradaic Efficiency

	Sn Load			Current Density, j			Flow/Area Ratio, Q/A			Curvature	
	Main Effect	Error	P^a	Main Effect	Error	P^a	Main Effect	Error	P^a	Center Point	P^a
$\bar{r}(-)$	0.810	0.02598	0	0.746	0.02598	0.015	0.146	0.02598	0.015	0.4367	0.005
$\bar{\eta}(-)$	1.174	0.04057	0	−0.219	0.04057	0.016	0.337	0.04057	0	0.6351	0.007

[a]Significant ($\alpha = 0.05$) if $P < 0.05$.

Additional experiments: Influence of j and Q/A at high Sn load

After analyzing the results of the factorial study, additional experiments were carried out in an attempt to improve process performance. As discussed previously, the best results were obtained with a high Sn load (i.e., 1.5 mg Sn cm^{-2}). Therefore, these additional experiments focused on further analyzing the influence of j and Q/A for a Sn load of 1.5 mg Sn cm^{-2}.

Additionally, because the Q/A ratio did not have a significant effect on rate or efficiency for a Sn load of 1.5 mg Sn cm^{-2}, a Q/A ratio of 0.57 mL min^{-1} cm^{-2} was used in these subsequent experiments. This low Q/A ratio allows for higher formate concentrations to be achieved. Finally, because the best results in the factorial experiments were obtained using the highest level of j, these additional experiments were designed to evaluate the performance of the process operating at even higher values of j.

Following a systematic approach similar to our previous work with metal plates,[26] additional experiments were performed using GDEs with 1.5 mg Sn cm^{-2} at various current densities higher than 32 mA cm^{-2} (j = 40, 60, 90 mA cm^{-2}) using a constant $Q/A = 0.57$ mL min^{-1} cm^{-2}; the results obtained are summarized in Table 4.

The graphs included in Figure 4 can be used to analyze the influence of current density. It can be seen that increasing j up to 40 mA cm^{-2} resulted in a dramatic increase in the rate: the rate obtained at $j = 40$ mA cm^{-2} was approximately $1.5 \cdot 10^{-3}$ mol m^{-2} s^{-1}, nearly twice the rate at $j = 32$ mA cm^{-2} and 5 times the rate at $j = 12$ mA cm^{-2} (Figure 4a). The Faradaic efficiency of 70% at $j = 40$ mA cm^{-2} was noticeably higher than the efficiencies of approximately 50% observed with current densities of 12 and 32 mA cm^{-2}, as shown in Figure 4b. Figure 4 also clearly shows that the average rate of formate production did not improve in the experiments carried out at current densities higher than 40 mA cm^{-2}, remaining around $1.5 \cdot 10^{-3}$ mol m^{-2} s^{-1}. Additionally, the average Faradaic efficiency fell drastically as j was increased to 60 or 90 mA cm^{-2}. The behavior at high current densities could be due the utilization of excess electric charge for competitive reactions such as H_2 evolution rather than product (formate) production at current densities above 40 mA cm^{-2}, resulting in decreased Faradaic efficiencies. It should be noted that while this behavior was observed in previous studies with plate electrodes,[21,26] the

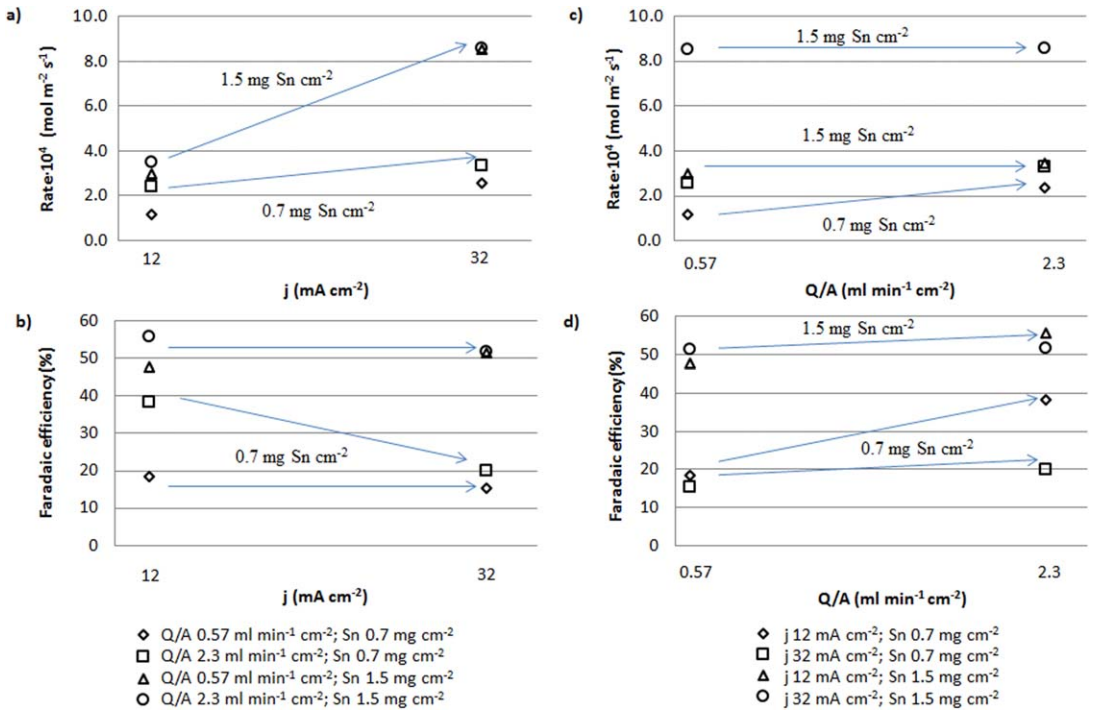

Figure 3. Formate rate and Faradaic efficiency at different *Q/A* ratios, current densities and Sn load.

a) Rate vs. current density, b) efficiency vs. current density, c) rate vs. *Q/A* ratio, d) efficiency vs. *Q/A* ratio. [Color figure can be viewed in the online issue, which is available at wileyonlinelibrary.com.]

Table 4. Additional Experiments at Higher Current Densities and Lower Q/A Ratio Using Sn Load = 1.5 mg Sn cm^{-2}

Current Density, j (mA cm^{-2})	Flow/area Ratio, Q/A (mL min^{-1} cm^{-2})	Measured Formate Concentration (mg L^{-1})	Average Rate·10^4 (mol m^{-2} s^{-1})	Rate SD·10^4 (mol m^{-2} s^{-1})	Faradaic Efficiency (%)	Faradaic Efficiency SD (%)	Cathode Potential vs. Ag/AgCl (V)	Cell Potential (absolute Value) (V)
40	0.57	692.0	14.6	±0.16	70.5	±0.8	−1.54	3.21
60	0.57	600.7	12.7	±4.60	40.8	±14.8	−2.02	4.17
90	0.57	673.8	14.2	±6.94	30.5	±14.9	−2.55	6.11
32	0.29	885.0	9.31	±9.51	56.1	±8.5	−1.52	3.22
40	0.29	1348.0	14.5	±0.08	69.9	±0.4	−1.63	3.17

threshold current densities for this behavior in plates were approximately four times lower than in GDEs (i.e., approximately 10 mA cm^{-2} in plate electrodes and 40 mA cm^{-2} in GDEs). Moreover, significant variability in the results was observed for the experiments carried out at the highest current densities (i.e., 60 and 90 mA cm^{-2}). This high variability could be attributed to electrode degradation at high current densities or may be associated with a lack of perfect homogeneity in the Sn particle dispersion during the fabrication of the electrode. The effects of this inhomogeneity may become more pronounced at higher current densities.

As mentioned previously, the analysis of the factorial design of experiments revealed that the influence of Q/A was very limited, and increasing Q/A did not significantly improve process performance. Accordingly, if an increase in Q/A does not allow for a higher formate production rate to be achieved, using higher Q/A ratios will simply dilute the product that is obtained. With this assumption, additional experiments were carried out to determine whether the Q/A ratio continued to have a limited influence at even lower Q/A ratios. Table 4 shows the results obtained for $Q/A = 0.29$ mL min^{-1} cm^{-2} (i.e., half of the lowest Q/A initially considered) at two different current densities (32 and 40 mA cm^{-2}). The rate and efficiency observed for $Q/A = 0.29$ mL min^{-1} cm^{-2} were very similar to those obtained for a higher Q/A (0.57 mL min^{-1} cm^{-2}). Consequently, the concentration of formate that was obtained doubled (from 404 to 885 ppm with $j = 32$ mA cm^{-2}, and from 692 to 1348 ppm with $j = 40$ mA cm^{-2}). These results confirmed that using low Q/A ratios in the Sn-GDE system generates a more concentrated product without sacrificing rate or efficiency. This conclusion is an interesting and novel finding that differs from results obtained in our previous work with Pb and Sn plates,[21,26] where the Q/A ratio had a greater influence on process performance. Using a Sn plate, increasing the Q/A improved both the rate and the Faradaic efficiency until an optimal Q/A (2.3 mL min^{-1} cm^{-2}) was reached; further increases above this optimal Q/A did not yield improved results.[26] This behavior was attributed to the fact that increasing the catholyte flow improved the supply of mass for electroreduction and, therefore, reduced mass transport limitations. This beneficial effect was observed until the catholyte flow became too high for the system, leading to dragging effects that decreased process performance and may explain the lower rates of formate production and Faradaic efficiency that were observed.[26] However, Sn-GDE did not show this trend. Unlike the trends observed for the plate electrodes, the trends reported in this work suggest that process performance may not be limited by external mass transport with Sn-GDEs. Due to the configuration of the GDE, the process may be affected only by internal diffusion limitations in the porous structure of the GDE where Sn particles are deposited. This could explain why process performance is hardly affected by catholyte flow.

Finally, results of formate rate production vs. Faradaic efficiency obtained at various experimental points, along with significant points for Sn plate electrodes obtained in previous studies,[21,26] are shown in Figure 5. This figure allows the performances of the Sn plate electrode and the GDE to be compared in terms of both efficiency and rate.

The most remarkable observation from Figure 5 is the increase in rate that can be achieved with the Sn-GDE. The maximum rate for the Sn plate electrode is $4.5 \cdot 10^{-4}$ mol m^{-2} s^{-1}, while the rate for the Sn-GDE is $1.4 \cdot 10^{-3}$ mol m^{-2} s^{-1}, a threefold increase. Moreover, this increase in rate is not accompanied by a loss in efficiency, as the maximum

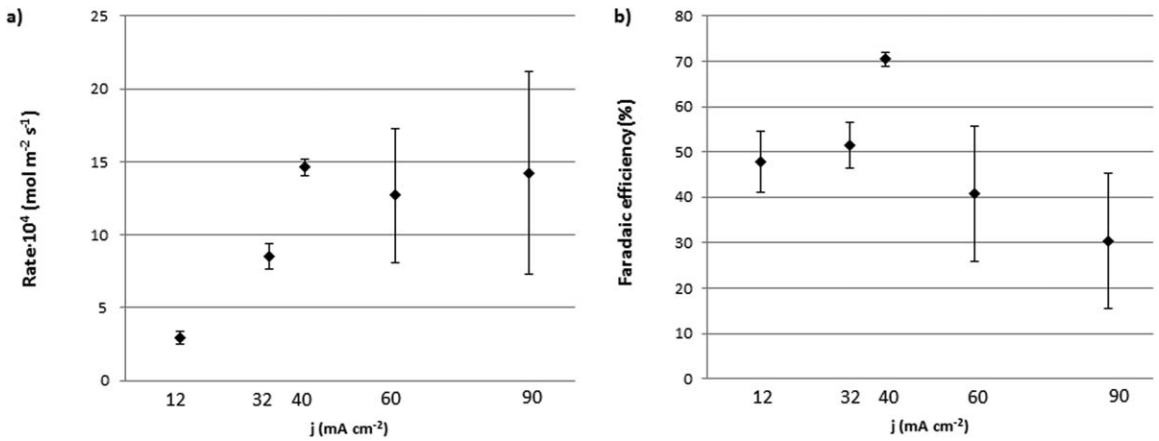

Figure 4. Formate rate (a) and Faradaic efficiency (b) at different current densities using $Q/A = 0.57$ mL min^{-1} cm^{-2} and GDE with 1.5 mg Sn cm^{-2}.

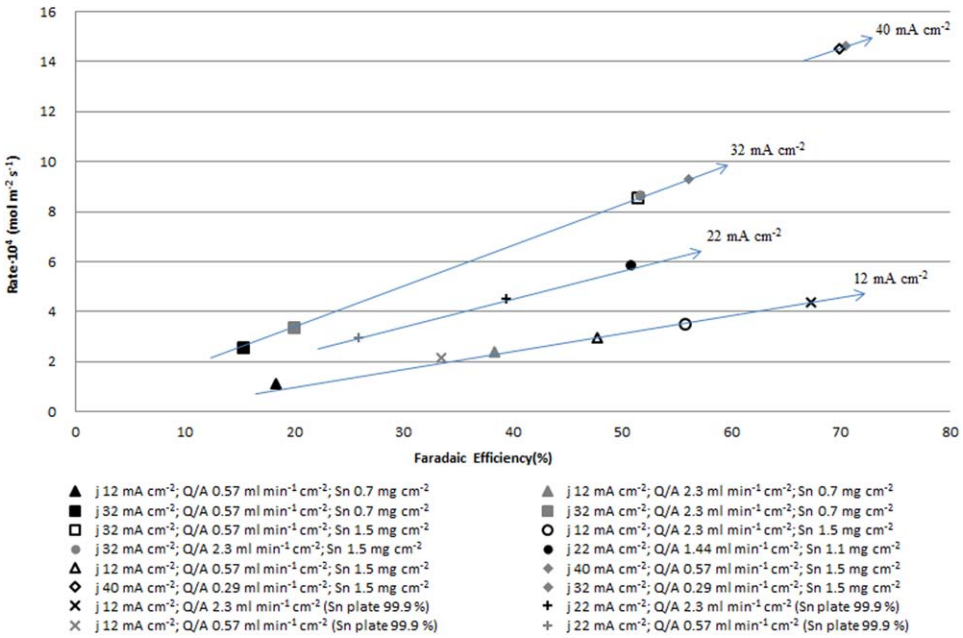

Figure 5. Relationship between the rate of formate production and Faradaic efficiency at the different experimental points studied.

[Color figure can be viewed in the online issue, which is available at wileyonlinelibrary.com.]

efficiencies obtained for both electrodes were approximately 70%, albeit at very different current densities. For the Sn plate electrode, a maximum efficiency of 67% was obtained at $j = 12$ mA cm^{-2}, while for the Sn-GDE, a maximum efficiency of 70% was obtained for $j = 40$ mA cm^{-2}. The ability to obtain the same efficiency at higher current densities highlights the fact that the GDE is able to work at higher current densities than Sn plate electrodes.

A similar trend in the performance of both GDEs and plate electrodes at $j = 12$ mA cm^{-2} can be observed. At such a low current density, increasing the Q/A ratio from 0.57 to 2.3 mL min^{-1} cm^{-2} resulted in a higher rate and efficiency for plates and GDEs, contrary to the behavior observed in GDEs at higher j. With $j = 12$ mA cm^{-2}, the Sn plate electrode achieved a rate of $4.36{\cdot}10^{-4}$ mol m^{-2} s^{-1} with an efficiency of 67%, while the GDE only reached a rate of $3.47{\cdot}10^{-4}$ mol m^{-2} s^{-1} with an efficiency of 55%.

However, when current density was increased to $j = 22$ mA cm^{-2}, the GDE exhibited better behavior than the Sn plate. The maximum rate for the GDE was $5.8{\cdot}10^{-4}$ mol m^{-2} s^{-1} with a 50% efficiency, while maximum rate for the plate at $j = 22$ mA cm^{-2} was $4.49{\cdot}10^{-4}$ mol m^{-2} s^{-1} with a lower efficiency of 39%.

Performance differences between the GDEs and plate electrodes become obvious at higher current densities. For plate electrodes, increasing the current density from $j = 12$ mA cm^{-2} to $j = 22$ mA cm^{-2} decreased the efficiency from 67 to 39%. However, the rate is largely unaffected, rising from 4.36 to $4.49{\cdot}10^{-4}$ mol m^{-2} s^{-1}. Conversely, the same increase in j for GDE electrodes slightly decreased the efficiency from 56 to 51% but significantly increased the rate from 3.47·to $5.8{\cdot}10^{-4}$ mol m^{-2} s^{-1}, a nearly 70% increase in rate.

Unlike the behavior observed with Sn plates, further increases in j with Sn-GDEs maintain improved rate and efficiency, efficiency that even increases for $j = 40$ mA cm^{-2}. This observation is a remarkable finding of the present study, as these results indicate that the Sn-GDE is able to function at higher current densities than Sn plate electrodes, allowing for improved rates of formate production without sacrificing Faradaic efficiency. Taking into account these results and comparing the experimental points for both electrodes, the Sn-GDE is clearly better than the Sn plate electrode.

Conclusions

This work presents new experimental results on the influence of key variables on the performance of a continuous electroreduction process in a filter-press type electrochemical cell. The cell is designed to convert CO_2 to formate in aqueous solutions under ambient conditions using a GDE loaded with Sn particles.

Statistical analysis of a factorial design of experiments revealed a significant influence of Sn load on both rate and efficiency. In light of these results, further studies to improve process performance should explore a wider range of Sn loads to determine the optimum Sn load per area of electrode. Moreover, future work should also investigate the influence of the size of the Sn particles used as electrocatalysts in the GDE.

Because only small decreases in the efficiency of GDEs were observed when the current density was increased, the Sn-GDE can be operated at higher current densities than the Sn plate electrode while yielding higher efficiencies (i.e., an efficiency of 70% for a current density of 40 mA cm^{-2}).

The most remarkable points with Sn-GDE achieved rates over $1.4{\cdot}10^{-3}$ mol m^{-2} s^{-1} with an efficiency of 70%, representing a threefold increase in rate compared to Sn plate electrodes. In addition, higher concentrations (885 and 1348 mg L^{-1}) were obtained with the Sn-GDE. Therefore, these results show the potential of Sn as an electrode material for the conversion of CO_2 to formate by

electroreduction. The combination of high rate, concentration and efficiency demonstrate the superior performance of GDEs compared to plate electrodes and the great potential of GDEs for CO_2 valorization. Despite the promising results obtained in this work, more research is still required into process variability and stability at higher current densities. Improving the manufacturing of the electrode and the deposition of the particles as well as optimizing the size of Sn particles are possible strategies to overcome the current limitations. Additionally, there is the potential for improvements to the nature of the solvent, including using ionic liquids, or implementing the GDE on a polymer electrolyte membrane reactor to further improve process performance.

Acknowledgments

This work was conducted under the framework of the Spanish Ministry of Science and Innovation Project ENE2010-14828.

Literature Cited

1. Figueroa JD, Fout T, Plasynski S, McIlvried H, Srivastava RD. Advances in CO_2 capture technology-the U.S. Department of Energy's Carbon Sequestration Program. *Int J Greenh Gas Control*. 2008;2(1):9–20.
2. Riemer P. Greenhouse gas mitigation technologies, an overview of the CO_2 capture, storage and future activities of the IEA greenhouse gas R&D programme. *Energy Convers Manage*. 1996;37(6–8):665–670.
3. Terwel BW, Daamen DDL. Initial public reactions to carbon capture and storage (CCS): Differentiating general and local views. *Clim Policy*. 2012;12(3):288–300.
4. Terwel BW, ter Mors E, Daamen DDL. It's not only about safety: Beliefs and attitudes of 811 local residents regarding a CCS project in barendrecht. *Int J Greenh Gas Control*. 2012;9:41–51.
5. Upham P, Roberts T. Public perceptions of CCS: Emergent themes in pan-European focus groups and implications for communications. *Int J Greenh Gas Control*. 2011;5(5):1359–1367.
6. Jhong HR, Ma S, Kenis PJ. Electrochemical conversion of CO_2 to useful chemicals: Current status, remaining challenges, and future opportunities. *Curr Opin Chem Eng*. 2013;2:191–199.
7. Jiang Z, Xiao T, Kuznetsov VL, Edwards PP. Turning carbon dioxide into fuel. *Philos Trans R Soc*. 2010;368(1923):3343–3364.
8. Olah GA, Prakash GKS, Goeppert A. Anthropogenic chemical carbon cycle for a sustainable future. *J Am Chem Soc*. 2011;133(33):12881–12898.
9. Mikkelsen M, Jørgensen M, Krebs FC. The teraton challenge. A review of fixation and transformation of carbon dioxide. *Energy Environ Sci*. 2010;3(1):43–81.
10. Quadrelli EA, Centi G, Duplan J, Perathoner S. Carbon dioxide recycling: Emerging large-scale technologies with industrial potential. *ChemSusChem*. 2011;4(9):1194–1215.
11. Kuhl KP, Cave ER, Abram DN, Jaramillo TF. New insights into the electrochemical reduction of carbon dioxide on metallic copper surfaces. *Energy Environ Sci*. 2012;5(5):7050–7059.
12. Whipple DT, Kenis PJA. Prospects of CO_2 utilization via direct heterogeneous electrochemical reduction. *J Phys Chem Lett*. 2010;1(24):3451–3458.
13. Jitaru M, Lowy DA, Toma M, Toma BC, Oniciu L. Electrochemical reduction of carbon dioxide on flat metallic cathodes. *J Appl Electrochem*. 1997;27(8):875–889.
14. Sánchez-Sánchez CM, Montiel V, Tryk DA, Aldaz A, Fujishima A. Electrochemical approaches to alleviation of the problem of carbon dioxide accumulation. *Pure Appl Chem*. 2001;73(12):1917–1927.
15. Hori Y, Wakebe H, Tsukamoto T, Koga O. Electrocatalytic process of CO selectivity in electrochemical reduction of CO_2 at metal electrodes in aqueous media. *Electrochim Acta*. 1994;39(11–12):1833–1839.
16. Agarwal AS, Zhai Y, Hill D, Sridhar N. The electrochemical reduction of carbon dioxide to formate/formic acid: Engineering and economic feasibility. *ChemSusChem*. 2011;4(9):1301–1310.
17. Li H, Oloman C. Development of a continuous reactor for the electro-reduction of carbon dioxide to formate—part 1: Process variables. *J Appl Electrochem*. 2006;36(10):1105–1115.
18. Othmer D, Kirk R. Kirk-Othmer Encyclopedia of Chemical Technology. New York: Wiley, 2004.
19. Rees NV, Compton RG. Sustainable energy: a review of formic acid electrochemical fuel cells. *J Solid State Electrochem*. 2011;15(10):2095–2100.
20. Yu X, Pickup PG. Recent advances in direct formic acid fuel cells (DFAFC). *J Power Sources*. 2008;182(1):124–132.
21. Alvarez-Guerra M, Quintanilla S, Irabien A. Conversion of carbon dioxide into formate using a continuous electrochemical reduction process in a lead cathode. *Chem Eng J*. 2012;207–208:278–284.
22. Innocent B, Liaigre D, Pasquier D, Ropital F, Léger JM, Kokoh KB. Electro-reduction of carbon dioxide to formate on lead electrode in aqueous medium. *J Appl Electrochem*. 2009;39(2):227–232.
23. Subramanian K, Asokan K, Jeevarathinam D, Chandrasekaran M. Electrochemical membrane reactor for the reduction of carbon dioxide to formate. *J Appl Electrochem*. 2007;37(2):255–260.
24. Li H, Oloman C. The electro-reduction of carbon dioxide in a continuous reactor. *J Appl Electrochem*. 2005;35(10):955–965.
25. Li H, Oloman C. Development of a continuous reactor for the electro-reduction of carbon dioxide to formate—part 2: Scale-up. *J Appl Electrochem*. 2007;37(10):1107–1117.
26. Alvarez-Guerra M, Del Castillo A, Irabien A. Continuous electrochemical reduction of carbon dioxide into formate using a tin cathode: Comparison with lead cathode. *Chem Eng Res Des*. 2014;92:692–701.
27. Li A, Wang H, Han J, Liu L. Preparation of a Pb loaded gas diffusion electrode and its application to CO_2 electroreduction. *Front Chem Sci Eng*. 2012;6(4):381–388.
28. Whipple DT, Finke EC, Kenis PJA. Microfluidic reactor for the electrochemical reduction of carbon dioxide: The effect of pH. *Electrochem Solid State Lett*. 2010;13(9):B109–B111.
29. MacHunda RL, Ju H, Lee J. Electrocatalytic reduction of CO_2 gas at Sn based gas diffusion electrode. *Curr Appl Phys*. 2011;11(4):986–988.
30. MacHunda RL, Lee J, Lee J. Microstructural surface changes of electrodeposited Pb on gas diffusion electrode during electroreduction of gas-phase CO_2. *Surf Interface Anal*. 2010;42(6–7):564–567.
31. Aeshala LM, Rahman SU, Verma A. Effect of solid polymer electrolyte on electrochemical reduction of CO_2. *Sep Purif Tech*. 2012;94:131–137.
32. Narayanan SR, Haines B, Soler J, Valdez TI. Electrochemical conversion of carbon dioxide to formate in alkaline polymer electrolyte membrane cells. *J Electrochem Soc*. 2011;158(2):A167–A173.
33. Wu J, Risalvato FG, Sharma PP, Pellechia PJ, Ke F, Zhou X. Electrochemical reduction of carbon dioxide: II. Design, assembly, and performance of low temperature full electrochemical cells. *J Electrochem Soc*. 2013;160(9):F953–F957.
34. Agarwal A, Guan S, Hill D, Rode E, Sridhar N. Electrochemical conversion of carbon dioxide to useful products. In: *AIChE 2012—2012 AIChE Annual Meeting, Conference Proceedings*. Pittsburgh, 2012.
35. Guan S, Agarwal A, Rode E, Hill D, Sridhar N. 3-D tin-carbon fiber paper electrodes for electrochemically converting CO_2 to formate/formic acid. Ceram Trans. 2013;No. 241.
36. Hinogami R, Yotsuhashi S, Deguchi M, Zenitani Y, Hashiba H, Yamada Y. Electrochemical reduction of carbon dioxide using a copper rubeanate metal organic framework. *ECS Electrochem Lett*. 2012;1(4):H17–H19.
37. Prakash GKS, Viva FA, Olah GA. Electrochemical reduction of CO_2 over Sn-Nafion ® coated electrode for a fuel-cell-like device. *J Power Sources*. 2013;223:68–73.
38. Pletcher D, Walsh FC. *Industrial Electrochemistry*, 2nd ed. London: Chapman & Hall, 1990.
39. Montgomery DC. *Design and Analysis of Experiments*, *4th* ed. New York: Wiley, 1997.

Manuscript received Jan. 16, 2014, and revision received June 12, 2014.